H-Tunneling Exhibiting Unexpectedly Small Primary Kinetic Isotope Effects

José P. L. Roque,[1,2] Cláudio M. Nunes,*[,1] Peter R. Schreiner,[2] Rui Fausto[1,3]

[1]University of Coimbra, CQC-IMS, Department of Chemistry, 3004-535 Coimbra, Portugal
[2]Institute of Organic Chemistry, Justus Liebig University, Heinrich-Buff-Ring 17, 35392 Giessen, Germany
[3]Faculty Sciences and Letters, Department of Physics, Istanbul Kultur University, Bakirkoy, Istanbul 34158, Turkey

ABSTRACT

Probing quantum mechanical tunneling (QMT) in chemical reactions is crucial to understand and develop new possibilities of molecular design. Primary H/D kinetic isotopic effects (KIEs) beyond the semiclassical maximum values of 7–10 are commonly used to assess QMT contributions in one-step hydrogen transfer reactions, because H-atom QMT reactions are assumed to necessarily have large primary H/D KIEs. Nevertheless, we report here the discovery of a reaction model occurring exclusively by H-atom QMT with residual primary H/D KIEs. A 2-hydroxyphenylnitrene, generated in N_2 matrix, was found to isomerize to an imino-ketone via domino QMT involving sequential *anti* to *syn* OH-rotamerization (rate determining step) and [1,4]-H shift reactions. This domino QMT transformation was also observed in the OD deuterated sample, and unexpected primary H/D KIEs between 3 and 4 were measured at 3 to 20 K. Analogous residual primary H/D KIEs were found in the *anti* to *syn* OH-rotamerization QMT of 2-cyanophenol in N_2 matrix. Evidence suggest that the intriguing isotope-insensitive QMT observations arise due to the coupling between the cryogenic N_2 medium and the movement of H/D tunneling particles. Should a similar rationale be extrapolated to conventional solution conditions, then QMT may have been overlooked in many chemical reactions.

INTRODUCTION

Quantum mechanical tunneling (QMT), the ability of particles to permeate through potential energy barriers, has been known to increase reaction rates beyond the classical expectations.[1–3] More recently, it has been recognized that QMT can determine the outcome of chemical reactions, superseding the classical kinetic or thermodynamic control, and lead to products impossible to rationalize based on the classical transition state theory.[4–10] QMT is particularly prominent for reactions involving the displacement of light hydrogen atoms (or ions) because its probability decreases exponentially with the square root of the tunneling particle's mass.[1] Hence, QMT manifestations are important in fields like enzymatic and conventional catalytic C−H bond activation.[11–16]

Primary kinetic isotope effects (KIEs, *e.g.*, k_H/k_D) are commonly measured to probe QMT in chemical reactions. The semi-classical interpretation of primary H/D KIEs sets an upper limit of 7–10 for one-step hydrogen transfer reactions occurring at room temperature (corresponding to the maximum zero-point vibrational energy (ZPVE) difference).[17] The observation of larger primary H/D KIEs supports the occurrence of QMT, owing to the much greater QMT probability of protium vs. deuterium.[18–23] Nevertheless, it also must be acknowledge that residual primary H/D KIEs (within the semi-classical limit) for one-step hydrogen transfer reactions can hide QMT contributions. In a seminal work, Saunders *et al.* (1979) described that the elimination reaction (E2) of 2-phenylethyltrimethylammonium with hydroxide ion (Scheme 1) occurs around room temperature with significative contribution of QMT despite showing residual primary H/D KIE ≤ 6, which was explained by the coupling between the movement of heavy-atoms (C−C contraction and C−N stretching) with the movement of the protium or deuterium.[24,25] Possibly due to lack of further convincing evidence, residual primary H/D KIEs have been associated with QMT being absent, which implies that many QMT reactions may have been overlooked. Reviving this important subject, we report here the discovery of a reaction model occurring exclusively by H-atom QMT at cryogenic temperatures with a residual primary H/D KIE, which apparently arises from the coupling between heavy-atoms of the cryogenic medium and the movement of protium or deuterium.

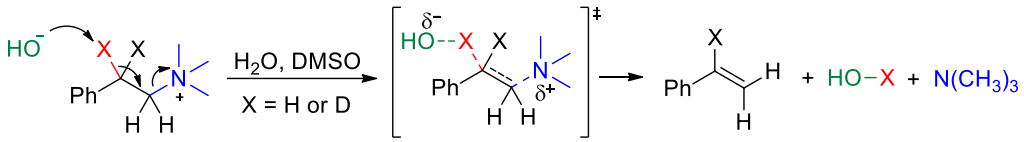

Scheme 1. Elimination reaction (E2) of 2-phenylethyltrimethylammonium with hydroxide ion in H_2O/DMSO (30-50%) at around room temperature. The existence of QMT contribution was supported by temperature-dependent KIE indicators (A_H/A_D and $E_a(D)–E_a(H)$ values) and found to be dependent on solvent composition. Residual primary H/D KIEs ≤ 6 were found.[24]

Unequivocal spectroscopic observations of QMT reactions have been obtained in the last decades using cryogenic matrices.[26–28] At cryogenic temperatures (*e.g.* 3−20 K) the activation of thermal over-the-barrier reactions (with energy barriers ≥ 4 kJ mol^{-1}) becomes virtually impossible and the occurrence of spontaneous transformations can only take place by vibrational ground-state QMT (deep tunneling). This approach has been decisive to unveil QMT in several organic reactions and to contribute to fundamental understandings on QMT chemistry.[5,29–31] In our recent endeavors to attain control over QMT reactivity, we have demonstrated an innovative strategy to switch ON a QMT reaction using external IR radiation. Upon generation of triplet 2-hydroxyphenylnitrene ^{3}**2** in an N_2 matrix at 10 K, its OH moiety converted from *anti* to *syn* orientation (^{3}**2a** to ^{3}**2s**) by selective vibrational excitation of the 2ν(OH) mode (Scheme 2).[32] This moves the H atom closer to the vicinal nitrene center and induces a fast H-atom QMT reaction to singlet imino-ketone **3Z**. Although ^{3}**2a** was kept essentially preserved in the dark during the experimental time scale of ~1 h, whereas more than half of it was consumed upon IR irradiation, for longer times an apparent slow spontaneous decay was noticed. Here, we present investigations revealing a spontaneous domino QMT process from ^{3}**2a** to **3Z**, and the surprising discovery that upon OD deuteration this QMT process does not cease. This and other OH-rotamerization QMT reaction models, investigated in cryogenic N_2 matrices, showed residual primary H/D KIEs. The origin of these unexpected results was addressed, bringing further knowledge and implications to QMT reactivity.

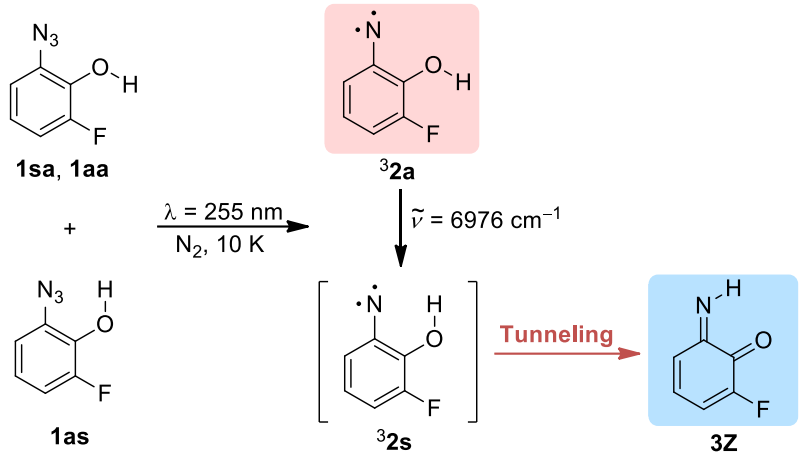

Scheme 2. Summary of the H-atom QMT activation from triplet 2-hydroxyphenylnitrene ^{3}**2** to imino-ketone **3Z** in an N_2 matrix at 10 K upon conformational isomerization of ^{3}**2a** to ^{3}**2s** by IR irradiation at the 2ν(OH) mode.[32]

RESULTS AND DISCUSSION

The arylazide **1** isolated in an N_2 matrix (Supporting Information, Figure S1 and Table S1) was photolyzed at 255 nm to generate the *anti*-OH triplet arylnitrene ^{3}**2a** (Figures S3 and S4). The imino-ketone **3Z** also formed (major product) during the irradiation (no other species was observed). The apparent prior observation of a slow spontaneous decay of ^{3}**2a** was then investigated by keeping the sample in the dark at 3.5 K. The IR spectrum collected at the end of 56 h reveals that more than half of ^{3}**2a** had transformed into **3Z** (Figure 1a,b). Characteristic IR bands of ^{3}**2a** were observed at ~3576 [ν(O−H)], 1538 [ν(CC)], 1444 [δ(C−H)], 996/990 [ν(C−F) + ν(CC)], and 768/765 [γ(C−H)] cm^{-1}, and of **3Z** at ~3216 [ν(N−H)], 1691 [ν(C=O)], 1114 [δ(N−H) + $\nu(C-C)_{as}$], 836 [δ(ring)], and 727 [γ(C−H)] cm^{-1}. The detailed assignment of the IR spectra of ^{3}**2a** and **3Z** (Tables S2 and S3) is in accordance with those previously reported.[32]

The kinetics of the spontaneous transformation of ^{3}**2a** to **3Z** in an N_2 matrix at 3.5 K in the dark was measured by collecting IR spectra over time using a longpass filter blocking light above 2200 cm^{-1} (Figure 2a). Fitting the experimental data with a first-order exponential decay equation provided a rate constant $k_{H(3.5K)} = 4.4 \times 10^{-6}$ s^{-1} [$\tau_{1/2}$ = 43.6 h] . The same procedure was performed to measure the kinetics at 10 and 20 K, and rate constants $k_{H(10K)} = 1.9 \times 10^{-5}$ s^{-1} [$\tau_{1/2}$ = 10.4 h] and

$k_{H(20K)} = 2.4 \times 10^{-5}$ s^{-1} [$\tau_{1/2}$ = 8.0 h] were obtained (Figure S5). The minimal increase in the reaction rate of ^{3}**2a** to **3Z** (less than one order of magnitude) observed upon increase the temperature up to ~5.7 times clearly indicates a QMT mechanism. The Arrhenius plot gives an activation energy of 6.1×10^{-2} kJ mol^{-1} and a pre-exponential factor of 3.6×10^{-5} s^{-1} (Figure S7). An activation energy close to zero and a pre-exponential factor similar to the rate constants emphasize the occurrence of a deep H-tunneling process.[33,34]

We then decided to investigate the effect of OD deuteration on the reactivity of triplet nitrene ^{3}**2**. The (OD) azide *d*-**1** with a deuterium enrichment of ~90% (see Experimental and Computational Methods in SI) was isolated in an N_2 matrix (Figure S2 and Table S1) and photolyzed at 255 nm to generate the *anti*-OD triplet nitrene *d*-^{3}**2a** (Figures S3 and S4). Similar to the photolysis of **1**, the photolysis of *d*-**1** led to (ND) imino-ketone *d*-**3Z** also formed (major product), and no evidence of the *syn*-OD triplet nitrene *d*-^{3}**2s** was found. Surprisingly, after keeping the irradiated sample in the dark at 3.5 K for 48 h, a significant amount of *d*-^{3}**2a** spontaneously transformed into *d*-**3Z** (Figure 1c,d). Distinctive IR bands of *d*-^{3}**2a** were observed at ~2644, 1440, 1306, 1074, and 902/897 cm^{-1}, in good agreement with the corresponding B3LYP/6-311+G(2d,p) computed IR bands at 2617 [ν(O−D)], 1432 [δ(C−H)], 1298 [ν(C−N)], 1064 [ν(C−F) + δ(O−D)], and 886 [δ(O−D)] cm^{-1}. Some representative bands of *d*-**3Z** were observed at ~2377, 1694, 1244, 1053, and 664 cm^{-1}, in good agreement with the corresponding B3LYP/6-311+G(2d,p) computed IR bands at 2352 [ν(N−D)], 1700 [ν(C=O)], 1230 [ν(C−F)], 1042 [$\nu(C-C)_{as}$ + δ(C−H)], and 666 [γ(N−D)] cm^{-1}. The comprehensive assignment of the IR spectra that clearly identifies *d*-^{3}**2a** and *d*-**3Z** is given in Tables S2 and S3.

The kinetics of the spontaneous transformation of *d*-^{3}**2a** into *d*-**3Z** in an N_2 matrix in the dark was then measured using fresh samples of *d*-^{3}**2a** generated at 3.5, 10, and 20 K. Following a similar procedure to that employed for the kinetics of the spontaneous transformation of ^{3}**2a** to **3Z**, rate constants $k_{D(3.5K)} = 1.5 \times 10^{-6}$ s^{-1} [$\tau_{1/2}$ = 131.1 h], $k_{D(10K)} = 4.2 \times 10^{-6}$ s^{-1} [$\tau_{1/2}$ = 46.1 h], and $k_{D(20K)} = 5.7 \times 10^{-6}$ s^{-1} [$\tau_{1/2}$ = 34.0 h] were obtained (Figures 2b and S6). Such marginal increase in the rate constants upon increasing the temperature up to ~5.7 times clearly indicates the existence of QMT also for the deuterated derivate (*d*-^{3}**2a** → *d*-**3Z**). The Arrhenius plot gives an activation energy of 4.7×10^{-2} kJ mol^{-1} and a pre-exponential factor of 7.5×10^{-6} s^{-1}, which strongly suggests a deep H-tunneling processes (Figure S7).

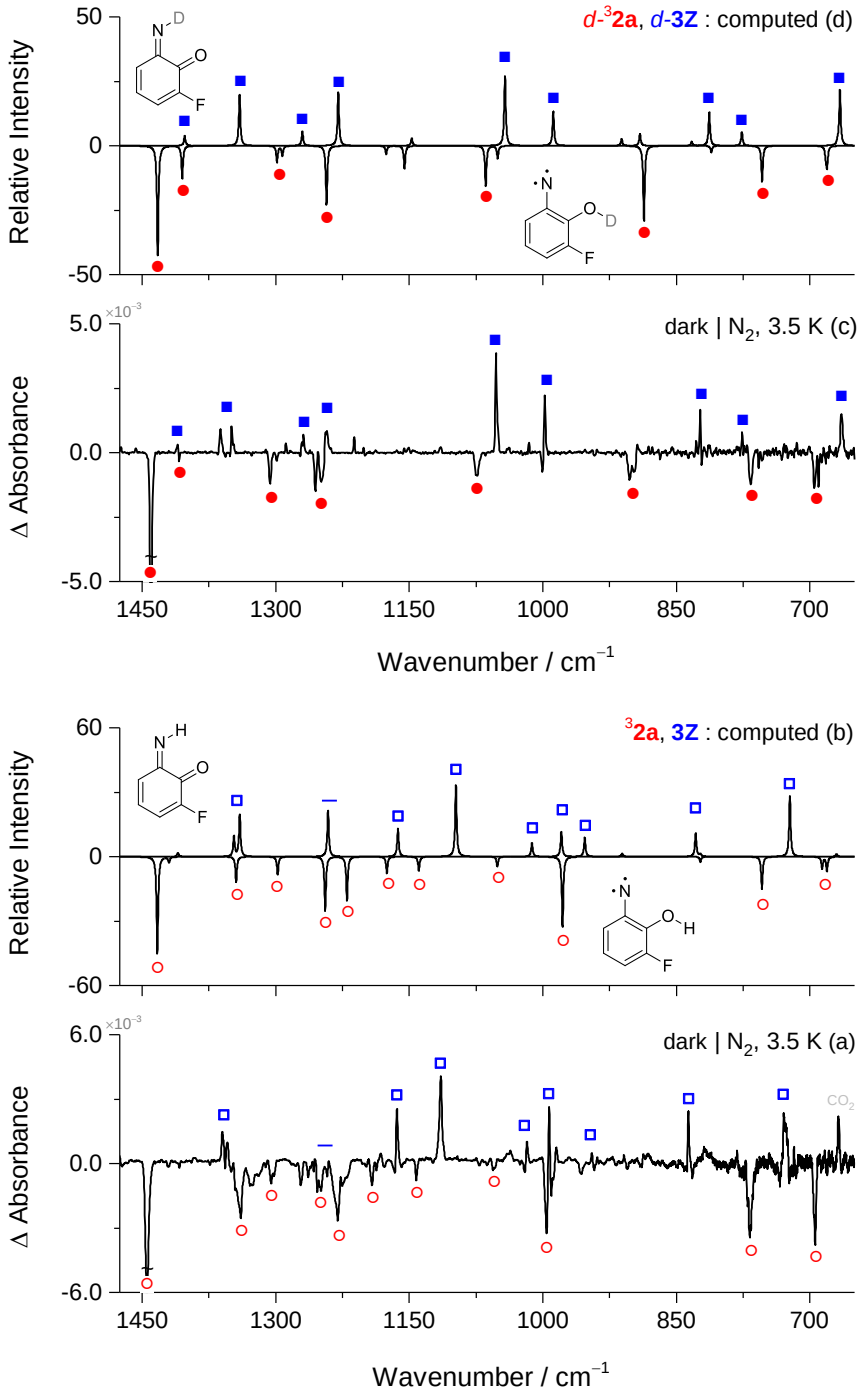

Figure 1. Experimental difference IR spectra showing the spontaneous transformation of (a) triplet *anti*-3-fluoro-2-hydroxyphenylnitrene ^{3}**2a** to (*Z*)-2-fluoro-6-imino-2,4-cyclohexadienone **3Z** after 56 h and of (c) deuterated (OD) *d*-^{3}**2a** to deuterated (ND) *d*-**3Z** after 48 h, in an N_2 matrix in the dark at 3.5 K (subsequent to irradiation of **1** and *d*-**1** at 255 nm, respectively). B3LYP/6-311+G(2d,p) computed IR spectrum of (b) ^{3}**2a** (pointing downwards) and **3Z** (pointing upwards), and of (d) *d*-^{3}**2a** (pointing downwards) and *d*-**3Z** (pointing upwards).

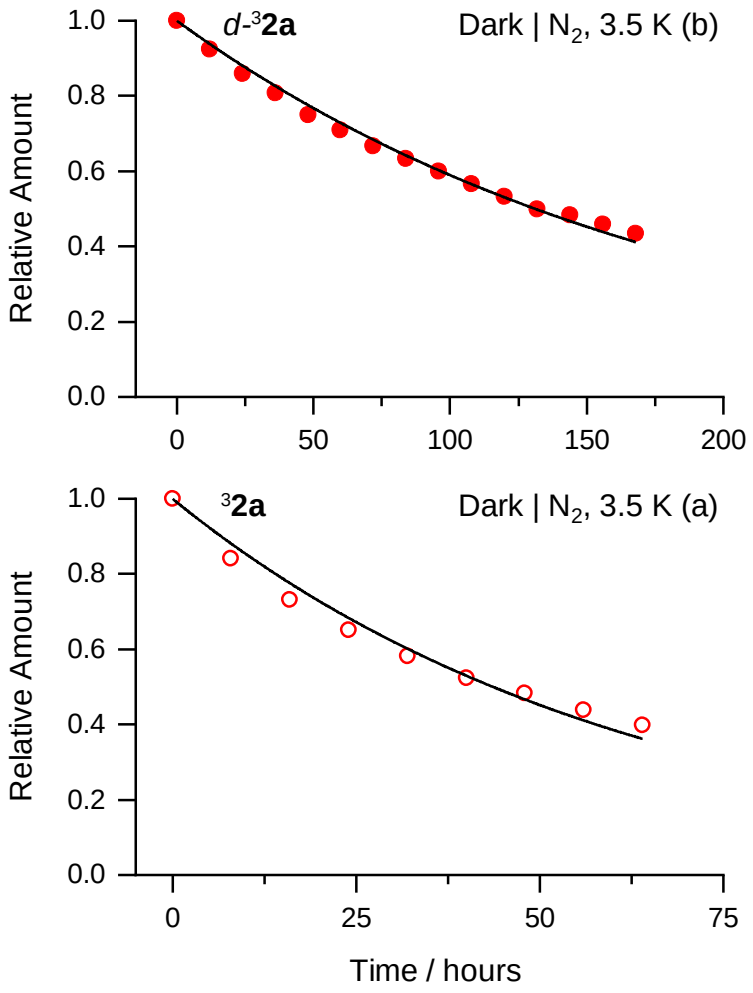

Figure 2. Kinetics of the spontaneous transformation (a) of triplet *anti*-3-fluoro-2-hydroxyphenylnitrene ^{3}**2a** to (*Z*)-2-fluoro-6-imino-2,4-cyclohexadienone **3Z**, and (b) of deuterated (OD) *d*-^{3}**2a** to deuterated (ND) *d*-**3Z**, in an N_2 matrix at 3.5 K in the dark. The IR spectra acquisition was performed with a long-pass filter transmitting only below 2200 cm^{-1}. The solid lines represent the best fits obtained using a first-order exponential decay. The rate constants obtained were $k_{H(3.5K)} = 4.4 \times 10^{-6}$ s^{-1} ($\tau_{1/2}$ = 43.6 h) and $k_{D(3.5K)} = 1.5 \times 10^{-6}$ s^{-1} ($\tau_{1/2}$ = 131.1 h).

The mechanism for the transformation of ^{3}**2a** to **3Z** must occur via a domino QMT process[35,36] involving sequential OH-rotamerization from ^{3}**2a** to ^{3}**2s** and [1,4]-H shift from ^{3}**2s** to **3Z** (Figure 3). The latter process must be considerably faster than the former because ^{3}**2s** is not detected experimentally. We found that the [1,4]-H shift QMT should occur through crossing the triplet ^{3}**2s** to the singlet **3Z** surfaces.[32] Although the minimum-energy crossing point (MECP) is relatively high in energy (≥39 kJ mol^{-1}, Table S4), the trajectory to reach the other side of the

surface should be very narrow, due to the huge reaction exothermicity (≥115 kJ mol^{-1}, Table S4), which makes H-atom QMT very fast. Considering that the rate-determining step must be the OH-rotamerization QMT from ^{3}**2a** to ^{3}**2s**, we analyzed this process in more detail.

Computations indicate that the OH-rotamerization of ^{3}**2a** to ^{3}**2s** has an energy barrier close to 19 kJ mol^{-1} and an exothermicity of ~3 kJ mol^{-1} (Figure 3 and Table S4). Similar results were found for the OD-rotamerization of *d*-^{3}**2a** to *d*-^{3}**2s** (~1 kJ mol^{-1} higher energy barrier). As mentioned above, experimental Arrhenius plots for the transformation of ^{3}**2a** to **3Z** and of *d*-^{3}**2a** to *d*-**3Z** give activation energies of 0.05-0.06 kJ mol^{-1} (Figure S7). The discrepancy between the computed energy barriers and the experimental activation energies allows us to confidently exclude any contribution from a classical over-the-barrier process. Applying the Wentzel−Kramers−Brillouin (WKB) model on the M06-2X/6-311+G(2d,p) computed reaction path of ^{3}**2a** to ^{3}**2s** and of *d*-^{3}**2a** to *d*-^{3}**2s**, OH and OD rotamerization QMT rates of 6.0 × 10^2 s^{-1} [$\tau_{1/2}$ = 1.2 ms] and 1.8 × 10^{-3} s^{-1} [$\tau_{1/2}$ = 7.4 min] were estimated (details are given in the Experimental and Computational Methods in SI).

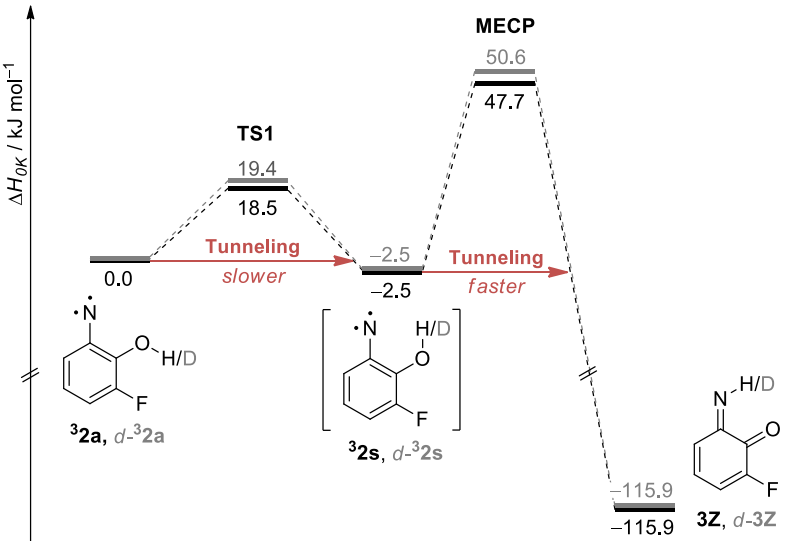

Figure 3. Relative energy diagram (ΔH_{0K} in kJ mol^{-1}) for the ^{3}**2a** → **3Z** and *d*-^{3}**2a** → *d*-**3Z** reactions, computed at the M06-2X/6-311+G(2d,p) + ZPVE level of theory. TS1 = Transition state; MECP = Minimum energy crossing point.

It has been reported that OH-rotamerization QMT rates (and other H-atom QMT processes) can decrease by two or more orders of magnitude when an N_2 matrix is used instead of Ar.[8,37–39]

Therefore, it is conceivable that the difference between our experimental and computed rates for the reaction of nitrene ^{3}**2a** and *d*-^{3}**2a** arises from an N_2 matrix solvation effect. Indeed, when azide **1** and *d*-**1** were isolated in Ar matrices at 10 K (Figures S1 and S2) and photolyzed at 255 nm, there was no evidence of trapped nitrenes ^{3}**2a** and *d*-^{3}**2a** by IR steady-state spectroscopy (a fast QMT process must occur with a half-time life less than a few seconds). However, as QMT rates decrease exponentially with the square root of the tunneling particle's mass, a massive deceleration should had occurred in the N_2 matrix experiments upon deuteration of the moving H-atom in the QMT process. For instance, the primary H/D kinetic isotope effect (KIE) computed with WKB approximation is 3.8×10^5. Therefore, the residual primary H/D KIE of 3.0 to 4.4 observed experimentally emerged at first sight as completely incomprehensible.

In an attempt to find a rationale for such intriguing residual primary H/D KIE, we carried out further investigations and revisited the OH-rotamerization QMT reaction of 2-cyanophenol **4**.[39] In agreement with the previously reported observations, the *anti*-OH **4a** (minor) and *syn*-OH **4s** (major) conformers were isolated in an N_2 matrix at 3.5 K (Figure S9), and the spontaneous transformation of **4a** to **4s** was observed in the dark (Figure 4a,b). Characteristic IR bands of **4a** appear at 3617 [ν(O−H)], 2240 [ν(C≡N)], 1590 [ν(CC)], 1506 [δ(C−H)], 1211 [δ(O−H) + ν(CC)], and 761/756 [γ(C−H)] cm^{-1}, and of **4s** at 3571 [ν(O−H)], 2230 [ν(C≡N)], 1580 [ν(CC)], 1492 [δ(C−H)], 1218 [δ(O−H) + ν(CC)], and 766/764 [γ(C−H)] cm^{-1} (comprehensive assignments are provided in Tables S5 and S6). The kinetics of this transformation was measured (see the Kinetics section in the SI for details) and has a rate constant of $k'_{H(3.5K)} = 3.1 \times 10^{-4}$ s^{-1} [$\tau_{1/2}$ = 37.6 min] (Figure 5a).[40] Previous measurements in N_2 matrices in the dark at 10, 15, and 20 K reported rate constants of ~3×10^{-4} s^{-1} [$\tau_{1/2}$ = 32−40 min].[39] These data unequivocally evidence the occurrence of OH-rotamerization QMT from **4a** to **4s** in the deep tunneling regime.

Subsequently, OD deuterated 2-cyanophenol *d*-**4** was prepared with an enrichment of ~90% (see Experimental and Computational Methods in SI). The sample was isolated in an N_2 matrix at 3.5 K as a mixture of *anti*-OD *d*-**4a** (minor) and *syn*-OD *d*-**4s** (major) conformers (Figure S10). After keeping the matrix in the dark for a few hours, *d*-**4a** also spontaneously had converted into *d*-**4s** (Figure 4c,d). Distinctive IR bands of *d*-**4a** were observed at 2670, 2240, 1501, 1266/1260, 928, and 760/756 cm^{-1}, in good correspondence with the corresponding B3LYP/6-311+G(2d,p) computed IR bands at 2645 [ν(O−D)], 2273 [ν(C≡N)], 1496 [δ(C−H)], 1250 [ν(C−O)], 916

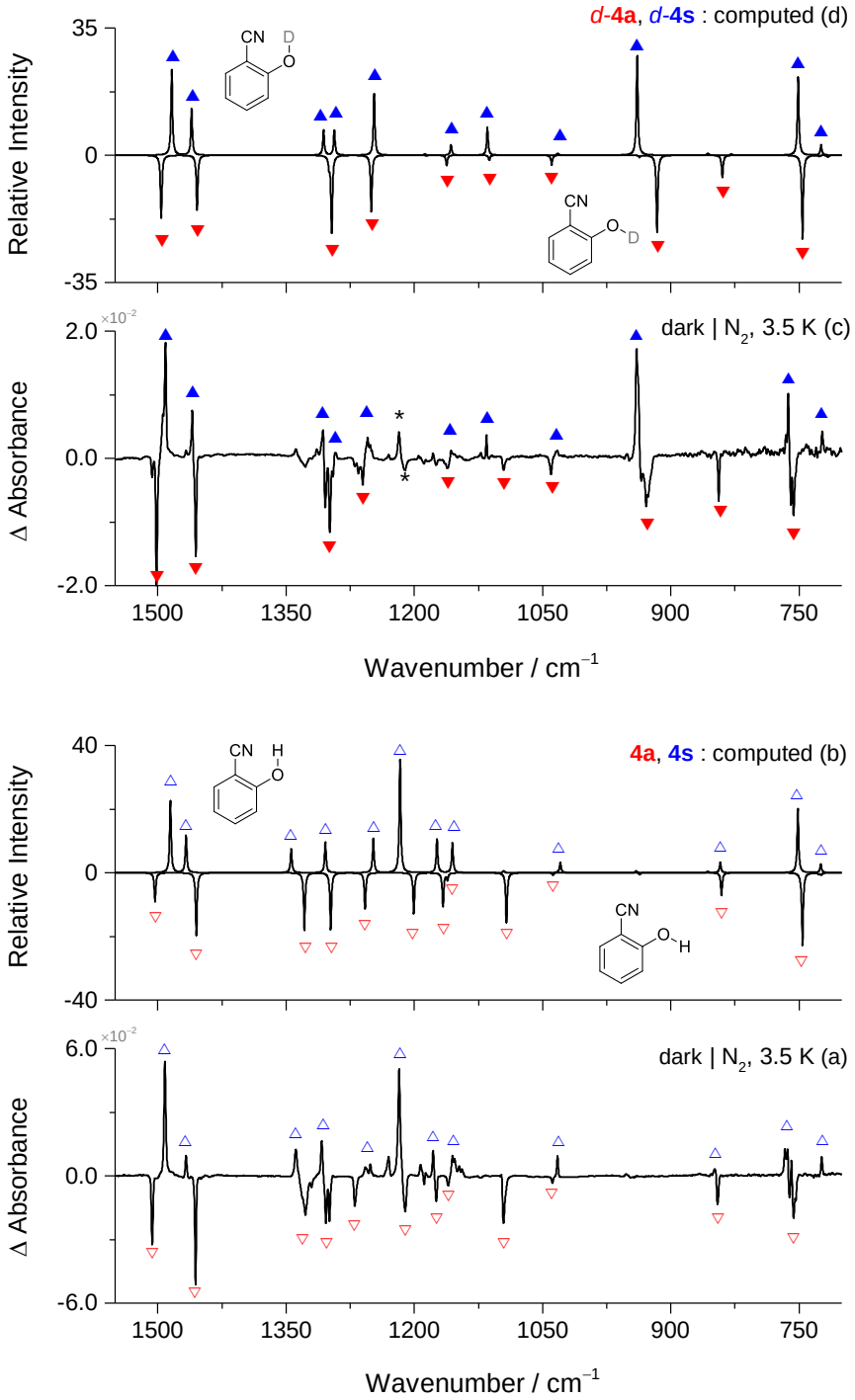

Figure 4. Experimental difference IR spectra showing the spontaneous transformation of (a) *anti*-2-cyanophenol **4a** to *syn*-2-cyanophenol **4s** after 2 h and of (c) deuterated (OD) *d*-**4a** to deuterated (OD) *d*-**4s** after 6 h, in an N_2 matrix in the dark. B3LYP/6-311+G(2d,p) computed IR spectrum of (b) **4a** (pointing downwards) and **4s** (pointing upwards), and of (d) *d*-**4a** (pointing downwards) and *d*-**4s** (pointing upwards).

[δ(O−D)], and 746 [γ(C−H)] cm^{-1}. Characteristic IR bands of *d*-**4s** observed at 2639, 2230, 1491,1255, 939, and 762 cm^{-1} compare well with the corresponding B3LYP/6-311+G(2d,p) computed IR bands at 2598 [ν(O−D)], 2255 [ν(C≡N)], 1484 [δ(C−H)], 1247 [ν(C−O)], 939 [δ(O−D)], and 751 [γ(C−H)] cm^{-1}. The kinetics of the *d*-**4a** to *d*-**4s** transformation was measured and gave a rate constant of $k'_{D(3.5K)} = 5.4 \times 10^{-5}$ s^{-1} [$\tau_{1/2}$ = 213.3 min] (Figure 5b).[40] Remarkably, these results demonstrate that the OD-rotamerization QMT of *d*-**4a** to *d*-**4s** occurs on a similar time scale as the OH-rotamerization QMT of **4a** to **4s**.

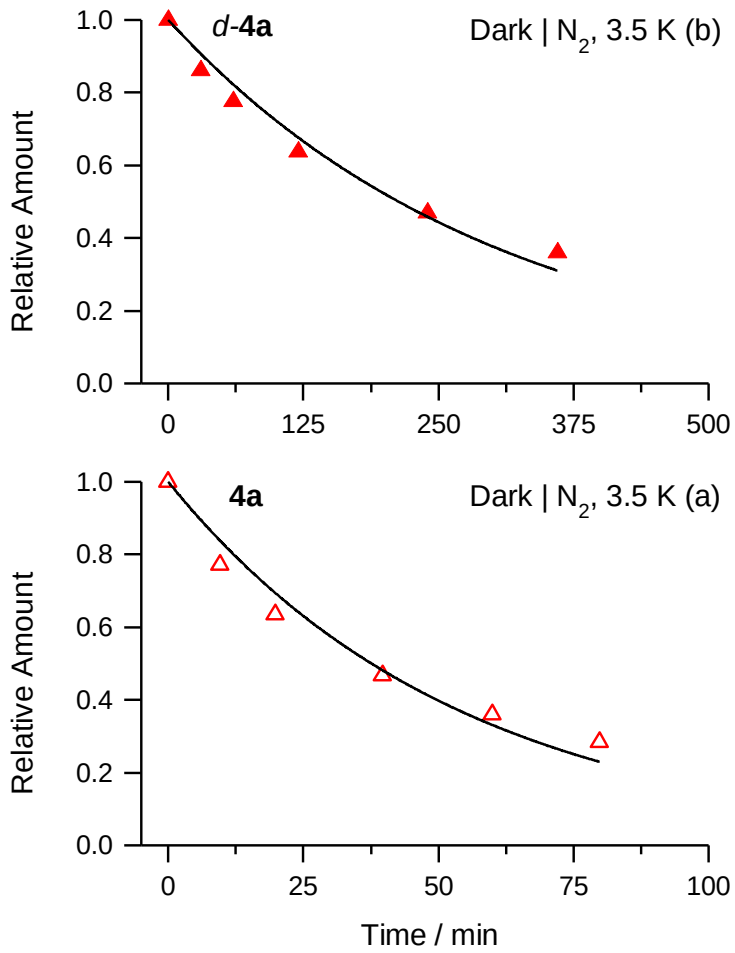

Figure 5. Kinetics of the spontaneous transformation (a) of *anti*-2-cyanophenol **4a** to *syn*-2-cyanophenol **4s**, and (b) of deuterated (OD) *d*-**4a** to deuterated (OD) *d*-**4s**, in an N_2 matrix at 3.5 K in the dark.[40] The IR spectra acquisition was performed with a long-pass filter transmitting only below 2200 cm^{-1}. The solid lines represent the best fits obtained using a first-order exponential decay. The rate constants obtained were $k'_{H(3.5K)} = 3.1 \times 10^{-4}$ s^{-1} ($\tau_{1/2}$ = 37.6 min) and $k'_{D(3.5K)} = 5.4 \times 10^{-5}$ s^{-1} ($\tau_{1/2}$ = 213.3 min).

Computations for the OH- and OD-rotamerizations of **4a** to **4s** and *d*-**4a** to *d*-**4s** show similar reaction barriers, 10.8 *vs* 11.5 kJ mol^{-1}, and an exothermicity of ~11 kJ mol^{-1} (Figure 6 and Table S7). Appling the WKB model on the M06-2X/6-311+G(2d,p) computed reaction path of **4a** to **4s** and of *d*-**4a** to *d*-**4s**, OH- and OD-rotamerization QMT rates of 4.4 × 10^{6} s^{-1} [$\tau_{1/2}$ ~ 0.2 μs] and 9.2 × 10^{2} s^{-1} [$\tau_{1/2}$ ~ 0.8 ms] were estimated (details are given in the Experimental and Computational Methods in SI). The computed fast QMT rates seem compatible with the lack of detection of *anti*-OH **4a** and *anti*-OD *d*-**4a** when experiments were carried out in Ar matrices at 3.5 K (Figures S9 and S10). As mentioned above, the use of the N_2 matrix medium is key to slow the OH-rotamerization QMT rates and make possible the experimental observation of **4a** (and *d*-**4a**) using steady state spectroscopy. However, the enormous QMT deceleration expected to occur upon deuteration (**4a** *vs* *d*-**4a**), with a computed H/D KIE of 4.8 × 10^{3} (based on the WKB approximation), conflicts with the unexpected residual primary H/D KIE of 5.7 derived experimentally. An inconsistency that is similar to that reported above for the QMT of triplet nitrene ^{3}**2a** and *d*-^{3}**2a**.

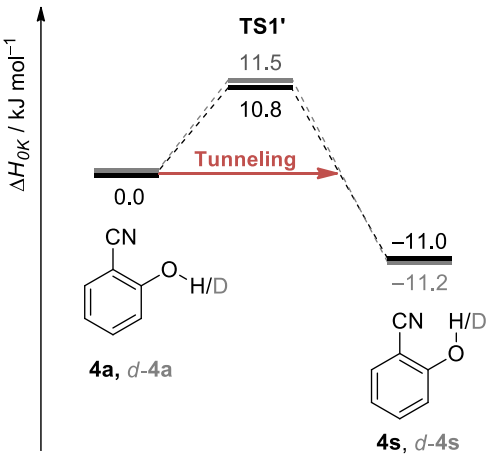

Figure 6. Relative energy diagram (ΔH_{0K} in kJ mol^{-1}) for the **4a** → **4s** and *d*-**4a** → *d*-**4s** reactions, computed at the M06-2X/6-311+G(2d,p) + ZPVE level of theory. TS1' = Transition state.

The OH- and OD-rotamerizations QMT rates were also computed using the more reliable small curvature tunneling (CVT + SCT) approximation.[41] Rate constants considering only the passage over-the-barrier were computed using the canonical variational transition state theory (CVT). The results from the CVT + SCT computations gave rate constants at 5 K similar to those

obtained from the WKB computations (Table S8). Moreover, the CVT + SCT and CVT rate constants computed for a wide range of temperatures clearly show the inexistence of thermally activated QMT for temperatures below 40 K (Figure 7). The computed huge H/D KIEs remains virtually unchanged from 5 to 40 K (~3×10^5 for arylnitrene ^{3}**2** and ~2×10^3 for cyanophenol **4**; similar to the values obtained using the WKB approximation) and only start to significantly decrease for temperatures above 60 K. Residual primary H/D KIEs (*e.g.*, < 7) are computed only as temperatures reach 110 K, where thermally activated QMT and thermal over-the-barrier reactivity are the dominant processes (Table S9). These data further support the hypothesis that the intriguing observed residual primary H/D KIEs in deep H-tunneling can only result from an N_2 matrix solvation effect.

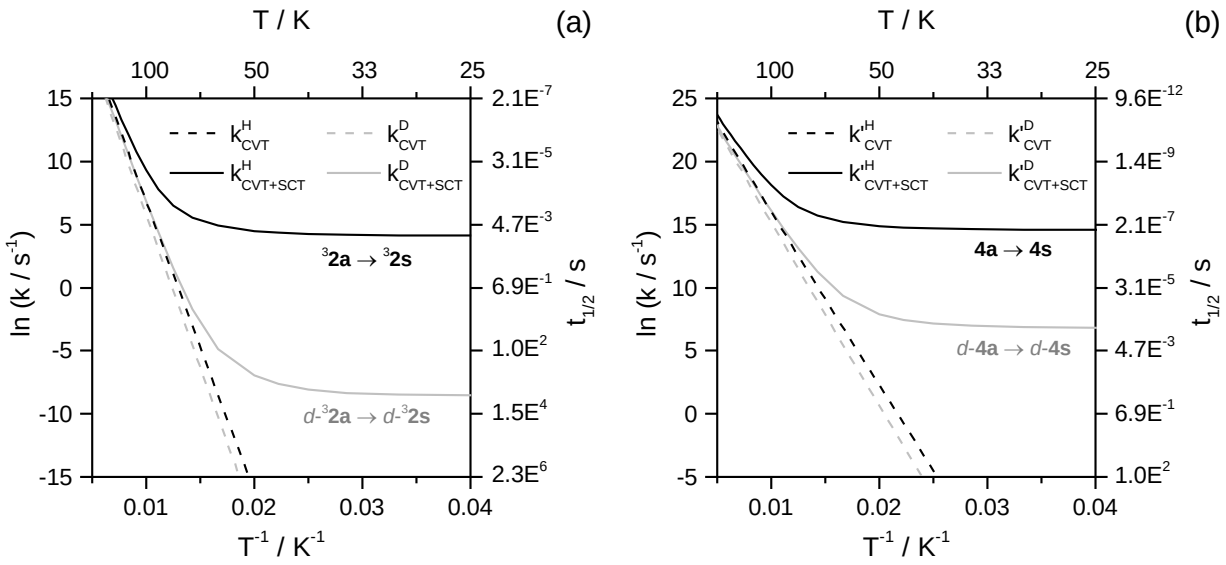

Figure 7. Arrhenius plots of the CVT (dashed lines) and CVT + SCT (full lines) rate constants computed at M06-2X/6-311+(2d,p) level of theory for (a) ^{3}**2a** → ^{3}**2s** (black) and ***d*-^{3}2a** → ***d*-^{3}2s** (gray), and (b) **4a** → **4s** (black) and *d*-**4a** → *d*-**4s** (gray).

The existence of R-OH···N_2-matrix interactions is well known and can be probed through the red-shift of the ν(OH) frequency.[42] For instance, when changing phenol and derivatives from an Ar to an N_2 matrix, a ν(OH) red-shift of 5−20 cm^{-1} was observed.[38,43,44] This type of interaction is also known to affect H-atom QMT reactions leading to a rate decrease.[8,37] For instance, when changing phenol derivatives from an Ar to an N_2 matrix, a significant decrease in the

OH-rotamerization QMT rates was observed, which was deemed crucial to allow the experimental characterization of their corresponding higher-energy conformers using steady-state IR spectroscopy.[38,39] Our present results unequivocally established that the solvation effects of the N_2 matrix can also lead to deep H-tunneling reactions with unexpected residual primary H/D KIEs. To the best of our knowledge, primary H/D KIEs for H-atom QMT reactions in N_2 matrices were previously only reported for the OH-rotamerization QMT of the HOCO radical, where also a surprising residual value of ~5 was found at 4.5 K.[45]

Seeking a rational for these intriguing findings, we analyzed some hypotheses that have been reported to address the influence of the medium on the QMT reactions. Specifically, (i) the existence of an isotope-insensitive process involving the medium in the formation of a pre-tunneling state for an H/D-transfer reaction,[46,47] (ii) the existence of an H/D-atom QMT reaction considering the sample interacting with the medium but decoupled from the motion of the medium,[48] (iii) the existence of dominant QMT gateways between specific resonant state pairs of the reactant and product with dependence on the medium.[49–52] However, as discussed in detail in the Supporting Information, none of these hypotheses help rationalize our experimental results. In all cases, the medium is assumed to affect QMT reactions only *indirectly*. We suggest instead that the nitrogen matrix medium should *directly* affect the QMT reaction by coupling with the migrating H/D atom of the sample, in resemblance with a hypothesis provided to rationalize the observations in the HOCO radical.[45] In that case, the motion of the heavier atoms of the medium that occurs concomitantly with the moving H/D atom can determine the QMT reaction rate. Such scenario may lead to QMT reactions significantly isotope-insensitive, thereby explaining our observed residual primary H/D KIEs (Figure 8).[53]

Interestingly, the computed stabilization that results from R-OH/OD···N_2 interactions (used as an approximate probe of the coupling between the sample and the medium) seems to correlate with the observed OH- and OD-rotamerization QMT rates in N_2 matrices (Table S11). The lower stabilization was found for the **4a**···N_2 complex [4.6 kJ mol^{-1} at the M06-2X/6-311+G(2d,p) level with D3 dispersion and counterpoise correction] that has the fastest QMT rate observed ($\tau_{1/2}$ = 37.6 min), whereas the higher stabilization was found for the *d*-^{3}**2a**···N_2 complex (5.1 kJ mol^{-1}) that has the slowest QMT rate observed ($\tau_{1/2}$ = 131.1 h). In the same vein, the hypothesis of the medium directly affecting QMT reactions by coupling with the migrating H/D atom of a sample seems also to justify the significant decrease in the primary H/D KIEs observed upon increasing the polarity

of the solvent in a particular organocatalytic reaction, which was recently discovered to proceed through significative QMT in its rate determining step.[54–59]

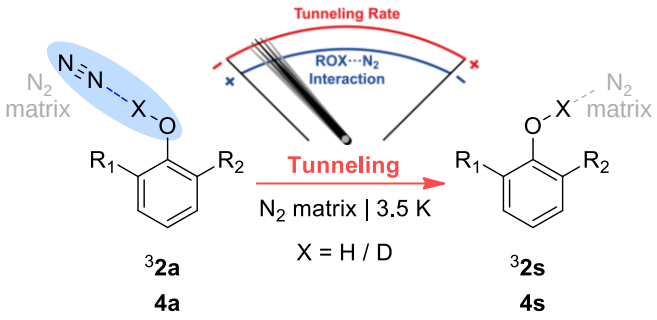

Figure 8. Representation of the coupling between the N_2 matrix medium and the migrating H/D atom in the phenol derivatives ^{3}**2a** and **4a** (represented specifically by considering the ROH/OD···N_2 interaction) leading to a significative reduction of the OH- and OD-rotamerization QMT rates and unusual residual primary H/D KIEs at cryogenic temperatures.

CONCLUSIONS

We demonstrated that triplet 2-hydroxyphenylnitrene ^{3}**2a** isomerizes to singlet imino-ketone **3Z** in cryogenic N_2 matrices via sequential OH-rotamerization (^{3}**2a** to ^{3}**2s**) and [1,4]-H shift (^{3}**2s** to **3Z**) QMT reactions. Albeit significantly more energetic, the latter process (involving triplet-to-singlet surface crossing) is considerably faster, which compromises the detection of ^{3}**2s**. This constitutes a rare and interesting example of a domino QMT reaction. Surprisingly, this domino QMT transformation was also found to proceed even with an OD deuterated sample (*d*-^{3}**2a** to *d*-**3Z**). Residual primary H/D KIEs between 3 to 4 were measured in N_2 matrices between 3 and 20 K. These results emerged as completely unexpected since a massive deceleration should have occurred upon doubling the tunneling particle's mass (QMT computations predict a primary H/D KIE of ~10^5 for the OH-rotamerization rate limiting step). Similar unexpected residual primary H/D KIEs were found for the OH-rotamerization QMT of 2-cyanophenol **4a** to **4s** in cryogenic N_2 matrices.

The use of a cryogenic N_2 matrix medium instead of noble-gas Ar matrix was crucial to capture the most energetic *anti*-OH conformers ^{3}**2a** and **4a**. The existence of R-OH···N_2-matrix interactions has been associated with a significant decrease of the OH-rotamerization QMT rates.

Our present results also demonstrate that the solvation effects of the N_2 matrix can lead to H-atom QMT reactions with residual primary H/D KIEs. These observations challenge the conventional belief that one-step hydrogen transfer QMT reactions occur necessarily with high primary H/D KIE values. We postulate that the coupling between the N_2 matrix medium and the migrating tunneling H/D-atom of the reactant directly affects QMT and is the rooting cause for significative isotope-insensitive QMT reactions. Based on this rationale, one can extrapolate similar scenarios to conventional solution conditions, where strong interactions between the solvent and the reactant can originate H-atom transfer reactions having significative QMT but residual primary H/D KIEs. Since primary H/D KIEs are typically used as a first indicator to search for H-atom QMT contributions, this puts into perspective the possibility of a systematic oversight of QMT in many chemical reactions.

ASSOCIATED CONTENT

All data is available in the main text or the supplementary information. The supplementary information (SI) includes: experimental and computational methods, further discussion about medium effects on QMT reactions, additional experimental and theoretical results, vibrational assignments, and computational data.

AUTHOR INFORMATION

Corresponding Author

*cmnunes@qui.uc.pt

Conflict of Interest

The authors declare no competing interests.

ACKNOWLEDGEMENTS

This work was supported by Project PTDC/QUI-QFI/1880/2020, funded by National Funds via the Portuguese Foundation for Science and Technology (FCT). The Coimbra Chemistry Centre –

Institute of Molecular Sciences (CQC-IMS) is supported by FCT through projects UIDB/00313/2020 and UIDP/00313/2020 co-funded by COMPETE and the IMS special complementary funds provided by FCT. C.M.N. acknowledges FCT for an Auxiliary Researcher grant. J.P.L.R. acknowledges FCT for a PhD (SFRH/BD/04467/2020) grant. The authors acknowledge the Laboratory for Advanced Computing at University of Coimbra (UC-LCA) for providing computing resources that have contributed to the research results reported within this paper, and LaserLab Coimbra for experimental facilities. This project has received funding from the European Research Council (ERC) under the European Union's Horizon 2020 research and innovation programme (Advanced Grant No. 101054751 "COLDOC" to P.R.S.). Views and opinions expressed are those of the authors only and do not necessarily reflect those of the European Union or the European Research Council. Nelson A. M. Pereira is acknowledged for the participation in preliminary experiments aiming the preparation of **1** and *d*-**1**.

REFERENCES

(1) Bell, R. P. *The Tunnel Effect in Chemistry*; Springer: Boston, MA, 1980.

(2) Miller, W. H. Tunneling Corrections to Unimolecular Rate Constants, with Application to Formaldehyde. *J. Am. Chem. Soc.* **1979**, *101*, 6810–6814.

(3) Garrett, B. C.; Truhlar, D. G. Accuracy of Tunneling Corrections to Transition State Theory for Thermal Rate Constants of Atom Transfer Reactions. *J. Phys. Chem.* **1979**, *83*, 200–203.

(4) Schreiner, P. R.; Reisenauer, H. P.; Ley, D.; Gerbig, D.; Wu, C.-H.; Allen, W. D. Methylhydroxycarbene: Tunneling Control of a Chemical Reaction. *Science.* **2011**, *332*, 1300–1303.

(5) Schreiner, P. R. Tunneling Control of Chemical Reactions: The Third Reactivity Paradigm. *J. Am. Chem. Soc.* **2017**, *139*, 15276–15283.

(6) Gerbig, D.; Schreiner, P. R. Formation of a Tunneling Product in the Photo-Rearrangement of o-Nitrobenzaldehyde. *Angew. Chem. Int. Ed.* **2017**, *56*, 9445–9448.

(7) Nunes, C. M.; Eckhardt, A. K.; Reva, I.; Fausto, R.; Schreiner, P. R. Competitive Nitrogen versus Carbon Tunneling. *J. Am. Chem. Soc.* **2019**, *141*, 14340–14348.

(8) Nunes, C. M.; Roque, J. P. L.; Doddipatla, S.; Wood, S. A.; McMahon, R. J.; Fausto, R. Simultaneous Tunneling Control in Conformer-Specific Reactions. *J. Am. Chem. Soc.* **2022**, *144*, 20866–20874

(9) Bae, S. H.; Li, X.-X.; Seo, M. S.; Lee, Y.-M.; Fukuzumi, S.; Nam, W. Tunneling Controls the Reaction Pathway in the Deformylation of Aldehydes by a Nonheme Iron(III)-Hydroperoxo Complex: Hydrogen Atom Abstraction versus Nucleophilic Addition. *J. Am. Chem. Soc.* **2019**, *141*, 7675–7679.

(10) Mandal, D.; Ramanan, R.; Usharani, D.; Janardanan, D.; Wang, B.; Shaik, S. How Does Tunneling Contribute to Counterintuitive H-Abstraction Reactivity of Nonheme Fe(IV)O Oxidants with Alkanes? *J. Am. Chem. Soc.* **2015**, *137*, 722–733.

(11) Klinman, J. P.; Kohen, A. Hydrogen Tunneling Links Protein Dynamics to Enzyme Catalysis. *Annu. Rev. Biochem.* **2013**, *82*, 471–496.

(12) Nagel, Z. D.; Klinman, J. P. Update 1 of: Tunneling and Dynamics in Enzymatic Hydride Transfer. *Chem. Rev.* **2010**, *110*, PR41–PR67.

(13) Klinman, J. P.; Offenbacher, A. R. Understanding Biological Hydrogen Transfer Through the Lens of Temperature Dependent Kinetic Isotope Effects. *Acc. Chem. Res.* **2018**, *51*, 1966–1974.

(14) Jin, J.; Zhao, Y.; Kyne, S. H.; Farshadfar, K.; Ariafard, A.; Chan, P. W. H. Copper(I)-Catalysed Site-Selective C(sp^3)–H Bond Chlorination of Ketones, (E)-Enones and Alkylbenzenes by Dichloramine-T. *Nat. Commun.* **2021**, *12*, 4065.

(15) Matxain, J. M.; Huertos, M. A., Hydrogen Tunneling in Stoichiometric and Catalytic Reactions involving Transition Metals. *ChemCatChem* **2023**, e202300962.

(16) Katoch, A.; Mandal, D. Effect of the Substituent on C-H Activation Catalyzed by a Non-Heme Fe(IV)O Complex: A Computational Investigation of Reactivity and Hydrogen Tunneling. *Dalt. Trans.* **2022**, *51*, 11641–11649.

(17) O'Ferrall, R. a. M. A Pictorial Representation of Zero-Point Energy and Tunnelling Contributions to Primary Hydrogen Isotope Effects. *J. Phys. Org. Chem.* **2010**, *23*, 572–579.

(18) Constantin, T.; Górski, B.; Tilby, M. J.; Chelli, S.; Juliá, F.; Llaveria, J.; Gillen, K. J.; Zipse, H.; Lakhdar, S.; Leonori, D. Halogen-Atom and Group Transfer Reactivity Enabled by

Hydrogen Tunneling. *Science.* **2022**, *377*, 1323–1328.

(19) Nakanishi, I.; Shoji, Y.; Ohkubo, K.; Ozawa, T.; Matsumoto, K. I.; Fukuzumi, S. A Large Kinetic Isotope Effect in the Reaction of Ascorbic Acid with 2-Phenyl-4,4,5,5-Tetramethylimidazoline-1-Oxyl 3-Oxide (PTIO˙) in Aqueous Buffer Solutions. *Chem. Commun.* **2020**, *56*, 11505–11507.

(20) Dhuri, S. N.; Lee, Y. M.; Seo, M. S.; Cho, J.; Narulkar, D. D.; Fukuzumi, S.; Nam, W. Mechanistic Insights into the Reactions of Hydride Transfer versus Hydrogen Atom Transfer by a Trans-Dioxoruthenium(VI) Complex. *Dalt. Trans.* **2015**, *44*, 7634–7642.

(21) Murata, S.; Tsubone, Y.; Tomioka, H. Large Deuterium Isotope Effects for Intramolecular CH Insertion Reaction of 2-Alkylphenylnitrenes. *Chem. Lett.* **1998**, 549–500.

(22) Lewandowska-Andralojc, A.; Grills, D. C.; Zhang, J.; Bullock, R. M.; Miyazawa, A.; Kawanishi, Y.; Fujita, E. Kinetic and Mechanistic Studies of Carbon-to-Metal Hydrogen Atom Transfer Involving Os-Centered Radicals: Evidence for Tunneling. *J. Am. Chem. Soc.* **2014**, *136*, 3572–3578.

(23) Large primary H/D KIEs might not be sufficient evidence of QMT in case of reactions with multiple steps, and temperature-dependent KIE indicators need to be investigated, *e.g.*, isotopic ratios of pre-exponential factors A_H/A_D or isotopic difference in the activation energies $E_a(D)–E_a(H)$. See for instance: Truong, P. T.; Miller, S. G.; Emily, E. J.; Bowring, M. A. Large Isotope Effects in Organometallic Chemistry. *Chem. Eur. J.* **2021**, *27*, 14800–14815.

(24) Kaldor, S. B.; Saunders, W. H. Mechanisms of Elimination Reactions. 30. The Contributions of Tunneling and Heavy-Atom Motion in the Reaction Coordinate to Deuterium Kinetic Isotope Effects in Eliminations from 2-Phenylethyl Derivatives. *J. Am. Chem. Soc.* **1979**, *101*, 7594–7599.

(25) Hama *et al.* also claim a QMT reaction with residual primary H/D KIEs, the addition of protium and deuterium atoms to benzene at cryogenic temperatures. However, in this case, the process of H/D surface diffusion is the rate-determining step and not the QMT reaction. See ref. 47.

(26) Nunes, C. M.; Reva, I.; Fausto, R. Direct Observation of Tunnelling Reactions by Matrix Isolation Spectroscopy. In *Tunnelling in Molecules: Nuclear Quantum Effects from Bio to*

Physical Chemistry; Kästner, J., Kozuch, S., Eds.; The Royal Society of Chemistry, 2021; pp 1–60.

(27) Schleif, T. Transformations of Strained Three-Membered Rings a Common, Yet Overlooked, Motif in Heavy-Atom Tunneling Reactions. *Chem. Eur. J.* **2022**, *28*, e202201775.

(28) Merini, M. P.; Schleif, T.; Sander, W. Heavy-Atom Tunneling in Bicyclo[4.1.0]Hepta-2,4,6-trienes. *Angew. Chem. Int. Ed.* **2023**, *62*, e202309717.

(29) Schreiner, P. R. Quantum Mechanical Tunneling Is Essential to Understanding Chemical Reactivity. *Trends Chem.* **2020**, *2*, 980–989.

(30) Henkel, S.; Merini, M. P.; Mendez-Vega, E.; Sander, W. Lewis Acid Catalyzed Heavy Atom Tunneling - the Case of 1H-Bicyclo[3.1.0]-Hexa-3,5-Dien-2-One. *Chem. Sci.* **2021**, *12*, 11013–11019.

(31) Fausto, R.; Ildiz, G. O.; Nunes, C. M. IR-Induced and Tunneling Reactions in Cryogenic Matrices: The (Incomplete) Story of a Successful Endeavor. *Chem. Soc. Rev.* **2022**, *51*, 2853–2872.

(32) Roque, J. P. L.; Nunes, C. M.; Viegas, L. P.; Pereira, N. A. M.; Pinho e Melo, T. M. V. D.; Schreiner, P. R.; Fausto, R. Switching on H-Tunneling through Conformational Control. *J. Am. Chem. Soc.* **2021**, *143*, 8266–8271.

(33) Fisher, J. J.; Michl, J. External and Internal Heavy-Atom Effects on the Rate of Spin-Forbidden Proton Tunneling in the Triplet Ground State Biradical, 1,3-Perinaphthadiyl. *J. Am. Chem. Soc.* **1987**, *109*, 583–584.

(34) Jonsson, T.; Glickman, M. H.; Sun, S.; Klinman, J. P. Experimental Evidence for Extensive Tunneling of Hydrogen in the Lipoxygenase Reaction: Implications for Enzyme Catalysis. *J. Am. Chem. Soc.* **1996**, *118*, 10319–10320.

(35) Schreiner, P. R.; Wagner, J. P.; Reisenauer, H. P.; Gerbig, D.; Ley, D.; Sarka, J.; Császár, A. G.; Vaughn, A.; Allen, W. D. Domino Tunneling. *J. Am. Chem. Soc.* **2015**, *137*, 7828–7834.

(36) Lohmiller, T.; Sarkar, S. K.; Tatchen, J.; Henkel, S.; Schleif, T.; Savitsky, A.; Sanchez-Garcia, E.; Sander, W. Sequential Hydrogen Tunneling in O-Tolylmethylene. *Chem. Eur. J.* **2021**, *27*, 17873–17879.

(37) Lopes, S.; Domanskaya, A. V; Fausto, R.; Räsänen, M.; Khriachtchev, L. Formic and Acetic Acids in a Nitrogen Matrix: Enhanced Stability of the Higher-Energy Conformer. *J. Chem. Phys.* **2010**, *133*, 144507.

(38) Lopes Jesus, A. J.; Reva, I.; Nunes, C. M.; Roque, J. P. L.; Pinto, S. M. V.; Fausto, R. Kinetically Unstable 2–Isocyanophenol Isolated in Cryogenic Matrices: Vibrational Excitation, Conformational Changes and Spontaneous Tunneling. *Chem. Phys. Lett.* **2020**, *747*, 137069.

(39) Lopes Jesus, A. J.; Nunes, C. M.; Reva, I.; Pinto, S. M. V.; Fausto, R. Effects of Entangled IR Radiation and Tunneling on the Conformational Interconversion of 2-Cyanophenol. *J. Phys. Chem. A* **2019**, *123*, 4396–4405.

(40) In the kinetic decay of **4a** and *d*-**4a**, the measurements were conducted during a time period where the sample amount decreases towards a plateau. The sample amount plateau was determined by leaving the sample in the dark for a much longer period, and this was assumed for simplification purposes to correspond to the total decay of the sample. More details are given in the Kinetics section of the Supporting Information.

(41) Fernandez-Ramos, A.; Ellingson, B. A.; Garrett, B. C.; Truhlar, D. G. Variational Transition State Theory with Multidimensional Tunneling. In *Reviews in Computational Chemistry*; Reviews in Computational Chemistry; 2007; pp 125–232.

(42) Fujii, A.; Miyazaki, M.; Ebata, T.; Mikami, N. Infrared Spectroscopy of the Phenol-N_2 Cluster in S_0 and D_0: Direct Evidence of the in-Plane Structure of the Cluster. *J. Chem. Phys.* **1999**, *110*, 11125–11128.

(43) Cao, Q.; Andrijchenko, N.; Ahola, A. E.; Domanskaya, A.; Räsänen, M.; Ermilov, A.; Nemukhin, A.; Khriachtchev, L. Interaction of Phenol with Xenon and Nitrogen: Spectroscopic and Computational Characterization. *J. Chem. Phys.* **2012**, *137*, 134305.

(44) Lopes Jesus, A. J.; de Lucena Júnior, J. R.; Fausto, R.; Reva, I. Infrared Spectra and Phototransformations of Meta-Fluorophenol Isolated in Argon and Nitrogen Matrices. *Molecules* **2022**, *27*, 8248.

(45) Ryazantsev, S. V.; Feldman, V. I.; Khriachtchev, L. Conformational Switching of HOCO Radical: Selective Vibrational Excitation and Hydrogen-Atom Tunneling. *J. Am. Chem. Soc.* **2017**, *139*, 9551–9557.

(46) Limbach, H. H.; Schowen, K. B.; Schowen, R. L. Heavy Atom Motions and Tunneling in Hydrogen Transfer Reactions: The Importance of the Pre-Tunneling State. *J. Phys. Org. Chem.* **2010**, *23*, 586–605.

(47) Hama, T.; Ueta, H.; Kouchi, A.; Watanabe, N. Quantum Tunneling Observed without Its Characteristic Large Kinetic Isotope Effects. *Proc. Natl. Acad. Sci. U. S. A.* **2015**, *112*, 7438–7443.

(48) Schleif, T.; Prado Merini, M.; Henkel, S.; Sander, W. Solvation Effects on Quantum Tunneling Reactions. *Acc. Chem. Res.* **2022**, *55*, 2180–2190.

(49) Choudhury, A.; DeVine, J. A.; Sinha, S.; Lau, J. A.; Kandratsenka, A.; Schwarzer, D.; Saalfrank, P.; Wodtke, A. M. Condensed Phase Isomerization through Tunneling Gateways. *Nature* **2022**, *612*, 691–695.

(50) Sinha, S.; Harlander, D.; Devine, J.; Choudhury, A.; Kandratsenka, A.; Saalfrank, P.; Schwarzer, D.; Wodtke, A. M. Manipulating Tunnelling Gateways in Condensed Phase Isomerization. *Nat. Sci.* **2023**, *3*, e20230006.

(51) Pettersson, M.; Maçôas, E. M. S.; Khriachtchev, L.; Lundell, J.; Fausto, R.; Räsänen, M. *Cis→trans* Conversion of Formic Acid by Dissipative Tunneling in Solid Rare Gases: Influence of Environment on the Tunneling Rate. *J. Chem. Phys.* **2002**, *117*, 9095–9098.

(52) Domanskaya, A.; Marushkevich, K.; Khriachtchev, L.; Räsänen, M. Spectroscopic Study of *Cis*-to-*Trans* Tunneling Reaction of HCOOD in Rare Gas Matrices. *J. Chem. Phys.* **2009**, *130*, 154509.

(53) A case could be made for the observation of H/D-atom QMT reactions with significant primary H/D KIE for molecules coupled to the N_2 matrix. Such a scenario must be observed if the motion of the H/D-atom determines the QMT rate, because this process is isotope-sensitive. At this stage, it is not obvious how to predict the occurrence of the scenario detailed in the text (rate determined mainly by the medium motion) or the above-mentioned alternative (rate determined mainly by H/D-atom motion).

(54) Xu, C.; Rao, V. U. B.; Weigen, J.; Loh, C. C. J. A Robust and Tunable Halogen Bond Organocatalyzed 2-Deoxyglycosylation Involving Quantum Tunneling. *Nat. Commun.* **2020**, *11*, 4911.

(55) Caldin *et al.* described in the 1970s that the abstraction of a proton from

4-nitrophenylnitromethane by strong bases occurs with tunneling contributions, in which the primary H/D KIEs decrease significatively upon increasing the polarity of the solvent. Likewise, they suggest that the motion of medium molecules should be coupled with the motion of the proton in the more polar solvents (refs. 56,57). However, latter reinvestigations showed that the measured KIEs were erroneous due to unrecognized loss of the isotopic label (refs. 58,59).

(56) Caldin, E. F.; Mateo, S. Kinetic Isotope Effects and Tunnelling in the Proton-Transfer Reaction between 4-Nitrophenylnitromethane and Tetramethylguanidine in Various Aprotic Solvents. *J. Chem. Soc. Faraday Trans. 1* **1975**, *71*, 1876–1904.

(57) Caldin, E. F.; Mateo, S. Kinetic Isotope Effects in Various Solvents for the Proton-Transfer Reactions of 4-Nitrophenylnitromethane with Bases. *J. Chem. Soc. Chem. Commun.* **1973**, 854–855.

(58) Kresge, A. J.; Powell, M. F. Rates of Hydrogen Exchange and Kinetic Isotope Effects in the Reaction of P-nitrophenylnitromethane with Amine Bases in Toluene Solution: Absence of Internal Return. *J. Phys. Org. Chem.* **1990**, *3*, 55–61.

(59) Caldin, E. F.; Mateo, S.; Warrick, P. Kinetics of the Reaction of (4-Nitrophenyl)Nitromethane with Tetramethylguanidine in Toluene. *J. Am. Chem. Soc.* **1981**, *103*, 202–204.